Isotope effect and gerade versus ungerade symmetry in HD predissociation revealed by the H(2*s*), H(2*p*), D(2*s*), and D(2*p*) fragments

Jie Wang and Yuxiang Mo*

Department of Physics, State Key Laboratory of Low-Dimensional Quantum Physics, Tsinghua University, Beijing 100084, China

(Received 21 May 2018; published 13 December 2018)

The isotope effect and the g-u symmetry in the HD predissociation have been studied by detecting the H(2s), H(2p), D(2s), and D(2p) fragments. For transitions to the $3p\pi D\ ^1\Pi_u^+(\upsilon=4)$, $4p\pi D'\ ^1\Pi_u^+(\upsilon=1)$, and $4p\sigma B''\ ^1\Sigma_u^+(\upsilon=2)$ states of HD, the branching ratios of the four dissociation channels, H(2s) + D(1s), H(2p) + D(1s), D(2s) + H(1s), and D(2p) + H(1s), were measured. Strong asymmetric distributions are found between the H(2s) + D(1s) and D(2s) + H(1s), and between the H(2p) + D(1s) and D(2p) + H(1s) channels. The results indicate the existence of g-u symmetry breaking as well as strong nonadiabatic couplings near the HD dissociation limits. However, the angular anisotropy parameters are found to be the same for the H(2s/2p) and D(2s/2p) fragments. In addition, the observed Beutler-Fano profiles in the H(2s/2p)- and D(2s/2p)-atom action spectra show no dependence on the H and D isotopes. This implies that the angular distribution of the fragments and the Beutler-Fano profiles are determined chiefly by the Franck-Condon transitions and are not affected by the g-u-state mixing.

DOI: 10.1103/PhysRevA.98.062509

I. INTRODUCTION

The hydrogen molecule has long served as a benchmark to study the electronic structure and dynamics of molecular systems. For H_2 and D_2, the electronic wave functions possess g-u inversion symmetry in the molecular frame. The g-u symmetry plays an important role in optical transitions and collision dynamics [1–9]. For HD, the g-u symmetry is still valid in the Born-Oppenheimer approximation that assumes the H and D have infinite masses. However, by taking into account the finite masses of H and D, the center-of-mass coordinate is no longer at the geometric center of the molecule. Because molecular spectra and dynamics are related to the center-of-mass coordinates, the g-u symmetry may be broken [1–17].

The g-u symmetry breaking in HD was first observed by Herzberg in the rotation-vibration spectrum [1]. Rovibrational transitions are forbidden for H_2 and D_2. Ubachs and coworkers measured accurate rotational energy levels of the $II'\ ^1\Pi_g$ state of HD [2–5], and it was found that the g-u interaction has to be taken into account in the theoretical calculations in order to obtain good agreement between the experimental and theoretical energy levels [3–7]. Recently, the g-u symmetry breaking has also been observed in the spectra of high-n Rydberg states of HD [11].

It is noted that the previous studies of g-u symmetry breaking mainly focused on the HD spectra. An alternative straightforward way to study the g-u symmetry is to detect the state-resolved H and D fragments from the HD photodissociation. If the g-u symmetry is conserved during the photodissociation process, the H and D atoms should play equivalent roles. For the predissociation of HD into the channels H(2s) + D(1s), H(2p) + D(1s), D(2s) + H(1s), and D(2p) + H(1s), one would expect that the H(2s) and H(2p) fragments have the same populations as the D(2s) and D(2p) fragments, respectively. On the other hand, if taking g-u interaction into account, one would expect the opposite results; i.e., the population of the H(2s) fragments is different from that of the D(2s) fragments, and the same is true of the H(2p) and D(2p) fragments. Furthermore, if the g-u-state mixing effect due to the different masses is taken into consideration in the calculation of potential energy curves, the D(2s/2p) + H(1s) channels correlate adiabatically to two u states and one g state ($3p\sigma B'\ ^1\Sigma_u^+$, $2p\pi C\ ^1\Pi_u$, and $GK\ ^1\Sigma_g^+$), whereas the H(2s/2p) + D(1s) channels correlate adiabatically to one u state and two g states ($2p\sigma B\ ^1\Sigma_u^+$, $II'\ ^1\Pi_g$, and $EF\ ^1\Sigma_g^+$) [2–7]. The dissociation limits for the D(2s/2p) + H(1s) channels are about 22 cm^{-1} higher than the H(2s/2p) + D(1s) channels because of the isotope effect. If the adiabatic correlations are preserved (in this case the g-u symmetries are totally broken near the dissociation limits), the photoexcitation to the u states in the Franck-Condon region should produce channels correlating to D(2s) + H(1s), D(2p) + H(1s), and H(2p) + D(1s). The channel H(2s) + D(1s) would not be observed.

There are many experimental and theoretical studies available on the predissociation dynamics of H_2 and D_2 [12–29]. For instance, the branching ratios, H(2s)/[H(2s) + H(2p)](α_H) and D(2s)/[D(2s) + (D(2p)](α_D), have been studied in great detail [18–29]. However, similar works on HD are rare. Durup [16] calculated the ratios between the H(2p) + D(1s) and D(2p) + H(1s) channels in the predissociation of HD and found that the former channel has more proportion, and the ratios change rapidly with the available energies (E_{avail}) in the threshold region. On the other hand,

*ymo@mail.tsinghua.edu.cn

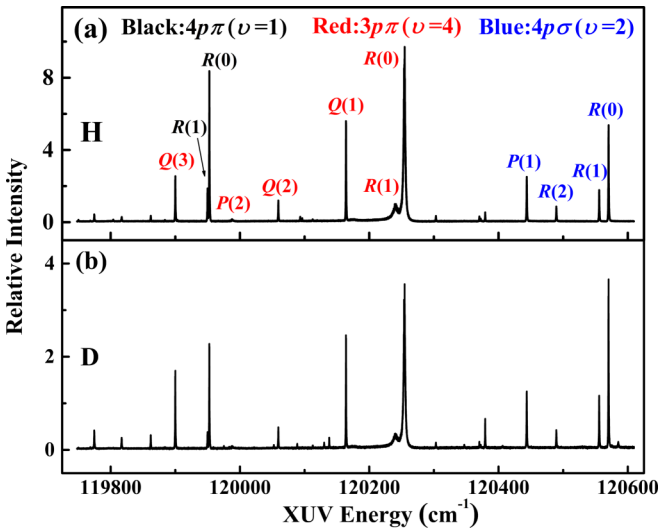

FIG. 1. The action spectra of (a) H($2s, 2p$), and (b) D($2s, 2p$) atoms from the predissociation of the $4p\pi D'\,{}^1\Pi_u(\upsilon = 1)$, $3p\pi D\,{}^1\Pi_u^{\pm}(\upsilon = 4)$, and $4p\sigma B''\,{}^1\Sigma_u^{+}(\upsilon = 2)$ states of the HD molecule. For the Q branches, some of the signals are due to the dissociative ionization induced by the probe laser [26–29]. The threshold for the lower dissociation limit, H($2s$) + D($1s$), is 118 664.8 cm^{-1} [12].

the $2s + 1s$ channels have fewer isotope effects. In Durup's calculation, only the vibronic couplings due to the isotope effect between the two states correlating to $1s + 2p\sigma$ were considered, and the predissociation mechanisms were not considered. The H($2p$)/D($2p$) branching ratios obtained in Durup's calculations are dependent only on the kinetic energies of the fragments. However, Durup's results are yet to be experimentally tested.

In addition to the product branching ratios among the H($2s$), H($2p$), D($2s$), and D($2p$) atoms, it should also be interesting to study if the angular distributions and absorption line profiles show dependences on the H and D fragments in the HD photodissociations. We believe that photodissociation of HD offers a rare opportunity to study both g-u symmetry breaking and vibronic coupling in molecules. Experimental measurements of the branching ratios α_{H}, α_{D} and the angular distribution of the fragments H($2s, 2p$) and D($2s, 2p$) can provide deep insights into the g-u symmetry breaking in HD as well as critical data for future theoretical calculations.

II. EXPERIMENTAL METHOD

The experimental setup consists of a tunable XUV laser pump (~10 nJ/pulse) and an UV laser probe system (365 nm, ~1 mJ/pulse), and a typical molecular beam machine equipped with a velocity map imaging component [26–29]. The tunable coherent XUV light was generated by four-wave sum mixing in a pulsed Kr jet. The α_{D} and α_{H} were determined by measuring the D($2s, 2p$) or H($2s, 2p$) signals as a function of the time delay between the XUV pump laser and the UV probe laser pulses under field-free condition (delay-time curve). The extraction electric field for the D^+ and H^+ ions was applied about 200 ns after the XUV laser pulse. The branching ratios α_{H} and α_{D} can be determined

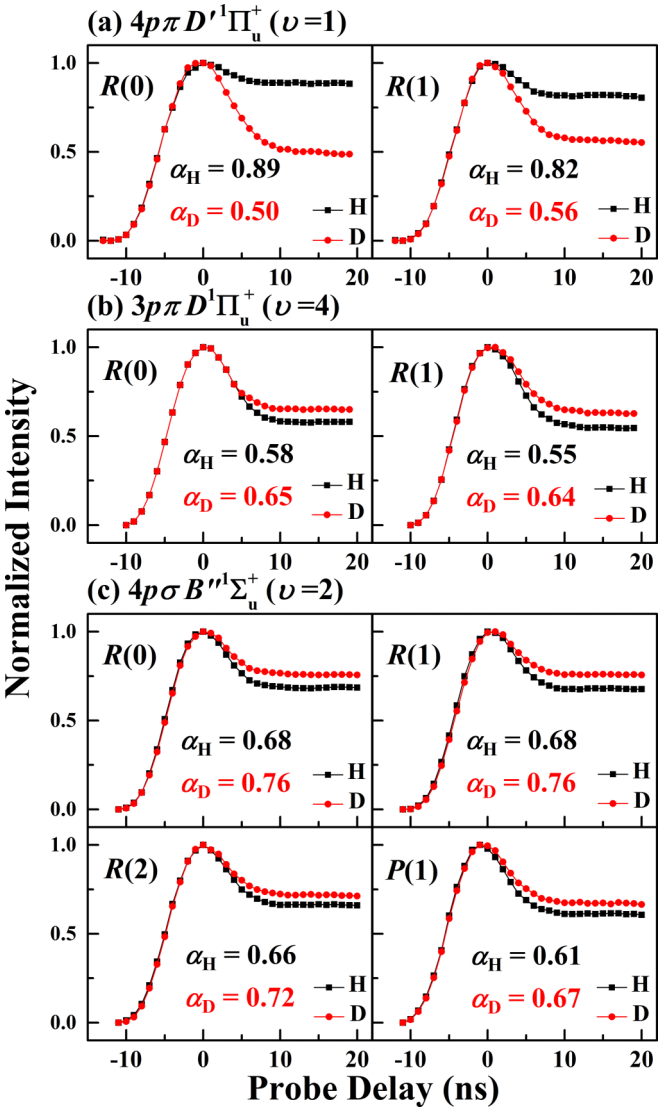

FIG. 2. The delay-time curves employed to determine the branching ratios H($2s$)/[H($2s$) + H($2p$)](α_{H}) and D($2s$)/[D($2s$) + D($2p$)](α_{D}) for the predissociation of HD.

using a simulation considering the lifetime of the $2s$ (0.14 s) and $2p$ (1.6 ns) states, and the temporal pulse widths of the pump and probe lasers (~6 ns) [26]. Note that the focus length of the lens for the probe laser beam was 300 mm, and the spot size at the focus was about 0.12 mm. The probe laser flux was estimated to be $\sim 2.7\times10^{27}$ photons/cm^2/s. The ionization cross section of the $2p$ state near the threshold is about 1.4×10^{-17} cm^2 [30]. The ionization rate of the $2p$ state is thus about 3.8×10^{10}/s. Therefore, the spontaneous decay of the $2p$ states (6.2×10^{8}/s) could be neglected in the detection [31].

The relative intensities ($\sigma_{\mathrm{H}}/\sigma_{\mathrm{D}}$) between the H($2s, 2p$) and the D($2s, 2p$) channels were determined by comparing their intensities in the fragment yield spectra. Employing α_{H}, α_{D}, and $\sigma_{\mathrm{H}}/\sigma_{\mathrm{D}}$ values, the branching ratios among the channels, H($2s$) + D($1s$), H($2p$) + D($1s$), D($2s$) + H($1s$), and D($2p$) + H($1s$), were determined. The purity of the HD sample was better than 98%.

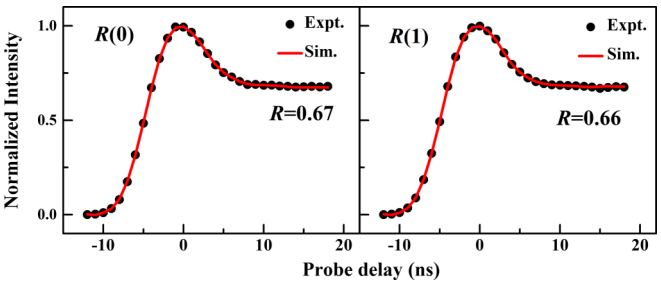

FIG. 3. The delay-time curves employed to determine the branching ratios $D(2s)/[D(2s)+D(2p)]$ for the predissociated states $4p\sigma\, B''\ ^1\Sigma_u^+(\upsilon=2)$ of D_2.

III. RESULTS AND DISCUSSION

A. Branching ratios among fragments H(2*s*), H(2*p*), D(2*s*), and D(2*p*)

Figures 1(a) and 1(b) show the fragment $H(2s, 2p)$ and $D(2s, 2p)$ intensities as a function of excitation photon energies (H- and D-atom action spectra), respectively. In the energy region of interest, there are three Rydberg states, $4p\pi\, D'\ ^1\Pi_u(\upsilon=1)$, $3p\pi\, D\ ^1\Pi_u(\upsilon=4)$, and $4p\sigma\, B''\ ^1\Sigma_u^+(\upsilon=2)$. It is clear in Figs. 1(a) and 1(b) that the spectra are almost identical if the scales of the y axis were neglected. For most of the peaks, the $H(2s, 2p)$ fragments have intensities about two times larger than those of the $D(2s, 2p)$ fragments.

Figures 2 and 3 show the delay-time curves to measure α_H and α_D of HD, and α_D of D_2, respectively. Table I lists the measured α_H and α_D of HD and the corresponding values of H_2 and D_2 for a comparison [26,29]. The overall branching ratios of the four channels are listed in Table II.

If the g-u symmetry is maintained in the predissociation of HD, the α_H and α_D of HD should be equal, which is apparently not true, as seen in Table I. For example, for the $R(0)$ and $R(1)$ transitions to $4p\pi\, D'\ ^1\Pi_u^+(\upsilon=1)$, the α_H of HD are 0.89 and 0.82, and are found to be appreciably larger than its α_D, 0.50 and 0.56, respectively, which indicate clearly that the g-u symmetry breaks down in the predissociations.

It is seen in Table I that there are more 2*s* components produced in the predissociation of $H_2/D_2/HD$. The reason

TABLE I. Relative branching ratios, $H(2s)/[H(2s)+H(2p)](\alpha_H)$ and $D(2s)/[D(2s)+D(2p)](\alpha_D)$, for the predissociation of H_2, D_2, and HD. The uncertainties are 0.03.

	H_2[a]	D_2[b]	HD	
	α_H	α_D	α_H	α_D
$4p\pi\, D'\ ^1\Pi_u^+$			$\upsilon=1$	
$R(0)$			0.89	0.50
$R(1)$			0.82	0.56
$3p\pi\, D\ ^1\Pi_u^+$	$\upsilon=3$	$\upsilon=4$	$\upsilon=4$	
$R(0)$	0.78	0.81	0.58	0.65
$R(1)$	0.81	0.82	0.55	0.64
$4p\sigma\, B''\ ^1\Sigma_u^+$	$\upsilon=1$	$\upsilon=2$	$\upsilon=2$	
$R(0)$	0.88	0.67	0.68	0.76
$R(1)$	0.85	0.66	0.68	0.76

[a]The data of H_2 are from Ref. [26].
[b]The data of D_2 for the transitions to the $3p\pi\, D\ ^1\Pi_u^+(\upsilon=4)$ states are from Ref. [29].

TABLE II. Branching ratios of the channels $H(2s)+D(1s)$, $H(2p)+D(1s)$, $D(2s)+H(1s)$, and $D(2p)+H(1s)$ for the predissociation of HD.

	Branching ratio			
Assignment	$H(2s)$[a]	$H(2p)$[a]	$D(2s)$[b]	$D(2p)$[b]
$4p\pi\, D'\ ^1\Pi_u^+(\upsilon=1)$				
$R(0)$	0.61	0.09	0.15	0.15
$R(1)$	0.62	0.14	0.13	0.11
$3p\pi\, D\ ^1\Pi_u^+(\upsilon=4)$				
$R(0)$	0.38	0.28	0.22	0.12
$R(1)$	0.37	0.30	0.22	0.12
$4p\sigma\, B''\ ^1\Sigma_u^+(\upsilon=2)$				
$R(0)$	0.45	0.21	0.26	0.08
$R(1)$	0.46	0.21	0.25	0.08
$R(2)$	0.44	0.22	0.24	0.10
$P(1)$	0.41	0.26	0.22	0.11

[a]The uncertainties of the branching ratios are 0.02 for $H(2s)$ and $H(2p)$.
[b]The uncertainties of the branching ratios are 0.01 for $D(2s)$ and $D(2p)$.

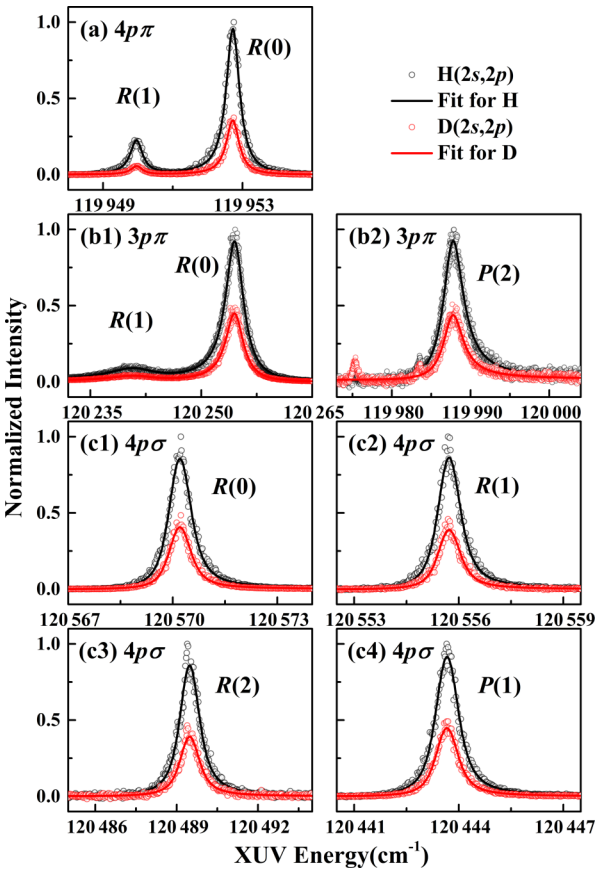

FIG. 4. Expanded $H(2s, 2p)$- and $D(2s, 2p)$-atom action spectra, (a) $4p\pi\, D'\ ^1\Pi_u(\upsilon=1)$, (b1), (b2) $3p\pi\, D\ ^1\Pi_u^+(\upsilon=4)$, and (c1)–(c4) $4p\sigma\, B''\ ^1\Sigma_u^+(\upsilon=2)$.

TABLE III. Line positions ω_0, linewidths Γ, Fano parameters q, branching ratios σ_H/σ_D $[H(2s,2p)+D(1s)]/[D(2s,2p)+H(1s)]$, and anisotropy parameters β_H and β_D for the predissociations of HD in the transitions of $4p\pi D'\ ^1\Pi_u(\upsilon=1)$, $3p\pi D\ ^1\Pi_u^{\pm}(\upsilon=4)$, and $4p\sigma B''\ ^1\Sigma_u^+(\upsilon=2) \leftarrow X\ ^1\Sigma_g^+(\upsilon=0)$.

	ω_0 (cm^{-1})							
Assignment	This work[a]	Δ[b]	Δ[c]	Γ[d]	q[e]	σ_H/σ_D[f]	β_H[g]	β_D[g]
$4p\pi D'\ ^1\Pi_u^+(\upsilon=1)$								
$R(0)$	119952.8	0.3				2.85	2.00	2.00
$R(1)$	119950.1	0.6				4.00	1.14	1.16
$3p\pi D\ ^1\Pi_u^{\pm}(\upsilon=4)$								
$R(0)$	120254.6	–0.1	0.0	2.9	–25	1.94	2.00	2.00
$R(1)$	120241.0	–0.3	0.7	7.6	–11	1.94	1.42	1.43
$P(2)$	119987.6	–0.2		3.0	12	1.90		
$Q(1)$	120164.0	–1.3	–0.5					
$Q(2)$	120059.4	0.6	–0.4					
$Q(3)$	119900.8	0.0	0.4					
$4p\sigma B''\ ^1\Sigma_u^+(\upsilon=2)$								
$R(0)$	120570.3	0.3		0.61	20	1.94	2.00	2.00
$R(1)$	120555.7	0.43		0.66	18	2.03	1.02	1.03
$R(2)$	120489.5	0.88		0.70	28	1.94	0.86	0.88
$P(1)$	120443.7	0.23		0.60	27	2.03	0.10	0.14

[a]Line positions determined by nonlinear fitting with uncertainties of 0.2 cm^{-1}.
[b]The difference between this work and Monfils [13].
[c]The difference between this work and Dickenson and Ubachs [15].
[d]With estimated uncertainties of 0.2 cm^{-1}.
[e]With estimated uncertainties of 6 for the $3p\pi D\ ^1\Pi_u^+(\upsilon=4)$ state and of 10 for the $4p\sigma B''\ ^1\Sigma_u^+(\upsilon=2)$ state.
[f]With estimated uncertainties of 0.10.
[g]With estimated uncertainties of 0.03.

for this is well understood [19–29] in the cases of H_2 and D_2. In the predissociation of the $3p\pi$ and $4p\sigma$ states, there is a coupling in the Franck-Condon region between the predissociated states with the $3p\sigma B'\ ^1\Sigma_u^+$ state that correlates with the $1s+2s$ channel. The $3p\sigma B'\ ^1\Sigma_u^+$ state is coupled with $2p\sigma B\ ^1\Sigma_u^+$ in the long range (~0.8 nm) that correlates with $1s+2p$. However, the predissociation from the $2p\sigma B\ ^1\Sigma_u^+$ state is believed to be less important. In the case of HD, the states $3p\sigma B'\ ^1\Sigma_u^+$ and $2p\sigma B\ ^1\Sigma_u^+$ in the Franck-Condon region correlate adiabatically with the $D(2s)+H(1s)$ and $H(2p)+D(1s)$ channels, respectively [5]. If the $3p\sigma B'\ ^1\Sigma_u^+$ and $2p\sigma B\ ^1\Sigma_u^+$ states are still the main dissociation channels in the predissociation of HD, as in the case of H_2 and D_2, the $D(2s)+H(1s)$ and $H(2p)+D(1s)$ channels should dominate the predissociations, which is not true as seen from Table II. This may indicate that the pairwise interaction among the g-u states changes the final state distributions. The details of the coupling mechanism should be studied in the future.

The overall branching ratios of the four channels, given in Table II, may provide a deeper insight into the predissociation dynamics of HD. Note that there are generally more $H(2s)$ or $H(2p)$ fragments produced than $D(2s)$ or $D(2p)$, respectively, indicating that the g-u symmetry breaks down in the predissociation. The theoretical calculations that include the coupling between the g and u states predicted the relative ratios $[H(2p)+D(1s)]/[D(2p)+H(1s)]$ [denoted as $H(2p)/D(2p)$] to be 2.1, 1.6, and 1.4, for $E_{avail}=720$, 1526, and 2332 cm^{-1} above the $D(2p)+H(1s)$ limit, respectively [16]. E_{avail}'s for the $R(0)$ and $R(1)$ transitions to $3p\pi D\ ^1\Pi_u^+(\upsilon=4)$ are ~1600 cm^{-1}, and the measured $H(2p)/D(2p)$ ratios are ~2.4, and the $H(2s)/D(2s)$ ratios are ~1.7. For the transition to $4p\sigma B''\ ^1\Sigma_u^+(\upsilon=2)$, E_{avail}'s for $R(0)$ and $R(1)$ transitions are ~1920 cm^{-1}, with measured $H(2p)/D(2p)$ ratios of ~2.6, and $H(2s)/D(2s)$, ~1.8. It is seen that the theoretical $H(2p)/D(2p)$ ratios are in semiquantitative agreement with the measurements.

It is interesting to note that the measured branching ratios for the $4p\pi D'\ ^1\Pi_u^+(\upsilon=1)$ state are very different from those of the $4p\sigma B''\ ^1\Sigma_u^+(\upsilon=2)$ and $3p\pi D\ ^1\Pi_u^+(\upsilon=4)$ states. The $H(2p)/D(2p)$ ratio for the $R(0)$ transition to $4p\pi D'\ ^1\Pi_u^+(\upsilon=1)$ is 0.60 with $E_{avail}\sim 1310\,cm^{-1}$, which is in disagreement with the theoretical prediction. Furthermore, the ratios $H(2s)/D(2s)$ are ~4.1, much larger those found for the $3p\pi D\ ^1\Pi_u^+(\upsilon=4)$ and $4p\sigma B\ ^1\Sigma_u^+(\upsilon=2)$ states. The latter result is also in disagreement with the theoretical prediction that the ratios $H(2s)/D(2s)$ are not significantly dependent on the available energies [16]. The values of α_H are larger than α_D in the predissociation of $4p\pi D'\ ^1\Pi_u^+(\upsilon=1)$, which is also in contrast with the results in the predissociation of $3p\pi D\ ^1\Pi_u^+(\upsilon=4)$ and $4p\sigma B\ ^1\Sigma_u^+(\upsilon=2)$. Therefore, it is seen that the branching ratios $H(2p)/D(2p)$ and $H(2s)/D(2s)$ depend not only on the available energies as predicted by the theoretical calculation [16] but also on the couplings between the predissociated states and the dissociative states. For the $4p\pi D'\ ^1\Pi_u^+(\upsilon=1)$ state, its predissociation mechanism is different from those of $3p\pi D\ ^1\Pi_u^+$ and $4p\sigma B''\ ^1\Sigma_u^+$, as discussed by Glass-Maujean [18]. The

predissociation of the $3p\pi\, D\ ^1\Pi_u^+$ and $4p\sigma\, B''\ ^1\Sigma_u^+$ states occurs mainly via direct coupling with the $3p\sigma\, B'\ ^1\Sigma_u^+$ states that in turn couple with the $2p\sigma\, B\ ^1\Sigma_u^+$ state, while the predissociation of the $4p\pi\, D'\ ^1\Pi_u^+(\upsilon = 1)$ state occurs in two different paths, coupling, respectively, with the $4p\sigma\, B''\ ^1\Sigma_u^+$ and $3p\pi\, D\ ^1\Pi_u^+$ states and the two states consequently coupling with $3p\sigma\, B'\ ^1\Sigma_u^+$ and $2p\sigma\, B\ ^1\Sigma_u^+$. Therefore, to fully account for our experimental data, all the g-u-state couplings should be taken into account as well as vibronic and l uncoupling among the predissociated and dissociative states [5].

B. Beutler-Fano profiles

In contrast with the product branching ratios that have strong g-u asymmetry, the predissociation line profiles and the fragment angular distributions show no dependence on the H and D fragments and thus maintain the g-u symmetry.

The expanded fragment yield spectra are shown in Fig. 4. The line profiles and hence the spectral parameters for the H$(2s, 2p)$ and D$(2s, 2p)$ fragments are found to be identical; that is, they are isotope independent. The line profiles are asymmetric due to the state interference in the predissociations, which are referred to as Beutler-Fano profiles. The predissociation of the $3p\pi\, D\ ^1\Pi_u^+$ state is mainly due to l uncoupling with the $3p\sigma\, B'\ ^1\Sigma_u^+$ state [13–25]. The spectral line profile is described by the Fano formula [32,33],

$$\sigma(\omega) \propto \frac{[q + 2(\omega - \omega_0)/\Gamma]^2}{1 + \left(\frac{2(\omega-\omega_0)}{\Gamma}\right)^2}. \tag{1}$$

This formula is usually applied to the photoabsorption spectrum, yet it can be still used if state-resolved and even angle-resolved fragments are detected in the predissociation [26–29]. In Eq. (1), q is the so-called Fano parameter, which relates the relative transition intensities from the ground state to $3p\pi\, D\ ^1\Pi_u^+$ and from the ground state to $3p\sigma\, B'\ ^1\Sigma_u^+$, and the interaction strength between the $3p\sigma\, B'\ ^1\Sigma_u^+$ and $3p\pi\, D\ ^1\Pi_u^+$ states. ω_0 is the resonance frequency. Γ represents the linewidth of the profile. There are mass scaling formulas of q and Γ based on $J \cdot l$ coupling, $q \propto \mu$ and $\Gamma \propto 1/\mu^2$, where μ is the reduced mass [14,15]. The values of μ are 1/2, 2/3, and 1 for H_2, HD, and D_2 molecules, respectively.

The parameters obtained by fitting the measured spectra using Eq. (1) are listed in Table III along with the relative signal intensities σ_H/σ_D. The observed line positions are in agreement with the reported values [13–15]. For transitions to $3p\pi\, D\ ^1\Pi_u^+(\upsilon = 4)$, based on earlier data from our group [27,29], it is known that $\Gamma(q)$ of $R(0)$ for H_2, HD, and D_2 are 4.8 (–14.4), 2.9 (–25), and 1.2 (–40), and for $R(1)$ are 13.3 (–10), 7.6 (–11), and 3.38 (–22), respectively, where Γ has unit of cm^{-1} and q is unitless. The corresponding ratios among H_2, HD, and D_2 are approximately in agreement with the theoretical ratios 4:2.25:1 for Γ and 3:4:6 for q, as mentioned above.

The resonance frequency ω_0 and the linewidth Γ are independent of the detected H and D fragments. This might indicate that these parameters are mainly dependent on the transitions in the Franck-Condon region. The g-u-state mixings in the dissociation limit region would not affect the two parameters.

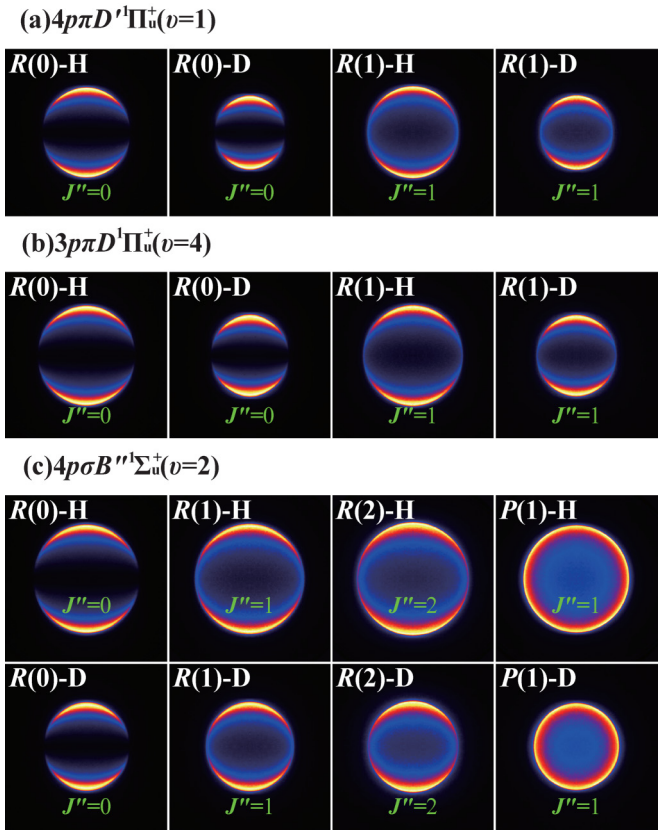

FIG. 5. Velocity map images of the H$(2s, 2p)$ and D$(2s, 2p)$ fragments from the predissociated states, (a) $4p\pi\, D'\ ^1\Pi_u^+(\upsilon = 1)$, (b) $3p\pi\, D\ ^1\Pi_u^+(\upsilon = 4)$, and (c) $4p\sigma\, B''\ ^1\Sigma_u^+(\upsilon = 2)$. The images were taken under electric fields with the pump and the probe laser pulses coincident in time. The polarization of the XUV laser was along the up-down direction. The corresponding angular distributions can be found in Fig. 6.

It is interesting to note that although the $P(2)$ and $R(0)$ transitions to the $3p\pi\, D\ ^1\Pi_u^+(\upsilon = 4)$ state reach the same final rotational state, $J = 1$, the q values for $P(2)$ and $R(0)$ transitions have opposite signs. This is due to the phase effect in the two-state coupling, and could be explained by the relationship derived using the Fano formula,

$$\frac{q[R(J'')]}{q[P(J''+2)]} = -\frac{J''+2}{J''+1}, \tag{2}$$

or $q[R(0)] : q[P(2)] = -2$ [29], which is in agreement with the measured ratio of -2.1.

For transitions to $4p\sigma\, B''\ ^1\Sigma_u^+$, it is seen in Table III that the linewidths of $4p\sigma\, B''\ ^1\Sigma_u^+$ are much smaller than those of $3p\pi\, D\ ^1\Pi_u^+$ and depend only slightly on the rotational quantum numbers, which indicate that the $4p\sigma\, B''\ ^1\Sigma_u^+$ and $3p\sigma\, B'\ ^1\Sigma_u^+$ states are vibronically coupled [18]. For transition to $4p\pi\, D'\ ^1\Pi_u^+$, the linewidth is smaller than the resolution of our instrument ($0.15\,cm^{-1}$). This suggests that the $4p\pi\, D'\ ^1\Pi_u^+$ state is weakly coupled to the dissociating continua, in agreement with the previous theoretical prediction [18].

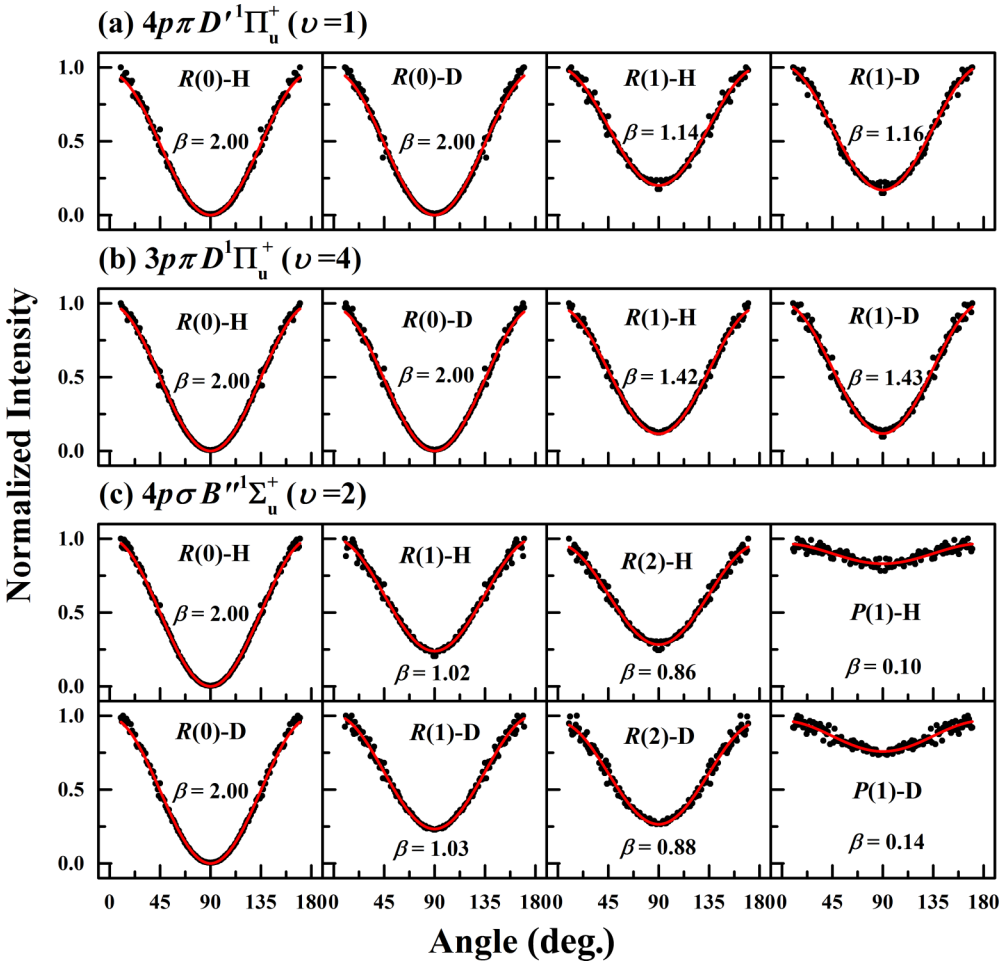

FIG. 6. The angular distributions of the H($2s, 2p$) and D($2s, 2p$) fragments extracted from the Abel transforms of the corresponding velocity map images shown in Fig. 5. The black dots in the figure are the experimental data, and the continuous curves are the nonlinear least-squares fittings using Eq. (3).

C. Fragment angular distributions

The angular distributions of the photofragments H($2s, 2p$) and D($2s, 2p$) have been measured. Figure 5 shows the velocity map images of the H and D fragments for transitions to the $4p\pi D'\,^1\Pi_u^+(\upsilon = 1)$, $3p\pi D\,^1\Pi_u^+(\upsilon = 4)$, and $4p\sigma B''\,^1\Sigma_u^+(\upsilon = 2)$ states. Figure 6 shows the corresponding angular distributions extracted from the images. The angular distributions of the fragments were fitted using the well-known formula

$$f(\theta) \propto 1 + \beta P_2(\cos\theta). \tag{3}$$

The β parameters are listed in Table III and are found to be essentially the same for the H($2s, 2p$) and D($2s, 2p$) fragments. It may thus be concluded that the angular distributions of the fragments depend only on the transitions in the Franck-Condon region and not on the g-u-state mixing near the dissociation limits.

The β values listed in Table III are in agreement with a model assuming a transition to a predissociating state of $^1\Sigma^+$ symmetry, in which $\beta = 2$, 1, 0.8, and 0 for the $R(0)$, $R(1)$, $R(2)$, and $P(1)$ transitions, respectively [26–29,34]. The measured angular distributions thus support the mechanism that the predissociating states are likely to be the $3p\sigma B'\,^1\Sigma_u^+$, $2p\sigma B\,^1\Sigma_u^+$, $EF\,^1\Sigma_g^+$, and $GK\,^1\Sigma_g^+$ states. The small differences between the predicted values from the model and the experimental values may be due to the interference effect in the predissociations [34].

IV. SUMMARY

We have studied the predissociation of HD and measured the branching ratios among the channels D($2s$) + H($1s$), D($2p$) + H($1s$), H($2s$) + D($1s$), and H($2p$) + D($1s$). The results show that the population ratios H($2s$)/D($2s$) and H($2p$)/D($2p$) are appreciably different from 1.0, which illustrate strong g-u-state mixings near the dissociation limits. On the other hand, the Beutler-Fano profiles and the angular distribution of the fragments show no isotope dependence, which indicates that these properties are not directly related to the g-u-state mixing. To reproduce our present experimental results, we suggest that future theoretical calculations should take all the g-u-state mixings, l uncouplings, and vibronic interactions into consideration. Future calculations should provide insights into the role of the g-u symmetry in HD photodissociation.

ACKNOWLEDGMENTS

We are grateful to Dr. Gabriel J. Vázquez of Universidad Nacional Autonóma de México for carefully reading the manuscript and making valuable suggestions. This work is funded by Projects No. 21833003 and No. 21773134 supported by the National Science Foundation of China and National Key R&D program of China (Grant No. 2018YFA0306504).

[1] G. Herzberg, Rotation-vibration spectrum of the HD molecule, Nature **166**, 563 (1950).

[2] I. Dabrowski and G. Herzberg, The absorption and emission spectra of HD in the vacuum ultraviolet, Can. J. Phys. **54**, 525 (1976).

[3] A. de Lange, E. Reinhold, W. Hogervorst, and W. Ubachs, Gerade/ungerade symmery-breaking in HD at the $n = 2$ dissociation limit, Can. J. Phys. **78**, 567 (2000).

[4] Th. G. P. Pielage, A. de Lange, F. Brandi, and W. Ubachs, Bound energy levels at the $n = 2$ dissociation threshold in HD, Chem. Phys. Lett. **366**, 583 (2002).

[5] A. de Lange, E. Reinhold, and W. Ubachs, Phenomena of g-u symmetry breakdown in HD, Int. Rev. Phys. Chem. **21**, 257 (2002).

[6] T. P. Grozdanov and R. McCarroll, Gerade-ungerade symmetry in HD: Bound states supported by the $I'^1\Pi_g$ outer potential well, J. Chem. Phys. **128**, 114317 (2008).

[7] T. P. Grozdanov and R. McCarroll, Gerade-ungerade symmetry breaking in bound states localized in the $II'\ ^1\Pi_g$ outer potential well of HD, Phys. Scr. **80**, 048123 (2009).

[8] K. Tsukiyama and Y. Ogi, The fluorescence lifetime of the gerade states of HD near the second dissociation limit, J. Mol. Spectrosc. **312**, 87 (2015).

[9] P. Pique, F. Hartmann, R. Bacis, S. Churassy, and J. B. Koffend, Hypefine-Induced Ungerade-Gerade Symmetry Breaking in a Homonuclear Diatomic Molecule near a Dissociation Limit: $^{127}I_2$ at the $^2P_{3/2}$-$^2P_{1/2}$ Limit, Phys. Rev. Lett. **52**, 267 (1984).

[10] E. Wells, B. D. Esry, K. D. Canes, and I. Ben-Itzhak, Asymmetric branching ratio for the dissociation of $HD^+(1s\sigma)$, Phys. Rev. A **62**, 062707 (2000).

[11] D. Sprecher and F. Merkt, Observation of g/u mixing in the high-n Rydberg states of HD, J. Chem. Phys. **140**, 124313 (2014).

[12] E. E. Eyler and N. Melikechi, Near-threshold continuum structure and dissociation energies of H_2, HD, and D_2, Phys. Rev. A **48**, R18 (1993).

[13] A. Monfils, The absorption spectra of the molecules H_2, HD, and D_2: Part VI. Rotational analysis of the B',B'',D,D', and D''states, J. Mol. Spectrosc. **15**, 265 (1965).

[14] M. Rothschild, H. Egger, R. T. Hawkins, J. Bokor, H. Pummer, and C. K. Rhodes, High-resolution spectroscopy of molecular hydrogen in the extreme ultraviolet region, Phys. Rev. A **23**, 206 (1981).

[15] G. D. Dickenson and W. Ubachs, The $D\ ^1\Pi_u$ state of HD and the mass scaling relation of its predissociation widths, J. Phys. B: At. Mol. Opt. Phys. **45**, 145101 (2012).

[16] J. Durup, On isotope effects in the predissociations of HD, J. Phys. (Paris) **39**, 941 (1978).

[17] T. I. Ivanov, G. D. Dickenson, M. Roudjane, N. de Oliveria, D. Joyeux, L. Nahon, W.-Ü. L. Tchang-Brillet, and W. Ubachs, Fourier-transform spectroscopy of HD in the vacuum ultraviolet at $\lambda = 87-112$ nm, Mol. Phys. **108**, 771 (2010).

[18] M. Glass-Maujean, Calculation of the predissociation probabilities of the $4p\pi\ ^1\Pi_u^+ \upsilon' \geqslant 1$ levels of H_2, Chem. Phys. Lett. **68**, 320 (1979).

[19] J. A. Beswick and M. Glass-Maujean, Interference effects on the H $(2p)$ to H $(2s)$ branching ratio in the photodissociation of hydrogen and Deuterium, Phys. Rev. A **35**, 3339 (1987).

[20] M. Glass-Maujean, H. Frohlich, and J. A. Beswick, Experimental Evidence of an Interference between Photodissociation Continua, Phys. Rev. Lett. **61**, 157 (1988).

[21] M. Glass-Maujean and J. A. Beswick, Coherence effects in the polarization of fluorescence emitted by photofragments: Application to H_2, Phys. Rev. A **38**, 5660 (1988).

[22] F. Mrugała, Predissociation of the $D\ ^1\Pi_u^+$ State of H_2 by photon impact, Mol. Phys. **65**, 377 (1988).

[23] H. Gao, Ch. Jungen, and C. H. Greene, Predissociation of H_2 in the $3p\pi\ D\ ^1\Pi_u^+$ state, Phys. Rev. A **47**, 4877 (1993).

[24] H. Gao, Predissociation of H_2 in the Rydberg states, J. Chem. Phys. **107**, 7278 (1997).

[25] J. Zs. Mezei, I. F Schneider, M. Glass-Maujean, and Ch. Jungen, Resonances in photoabsorption: predissociation line shapes in the $3p\pi\ D\ ^1\Pi_u^+ \leftarrow X\ ^1\Sigma_g^+$ system in H_2, J. Chem. Phys. **141**, 064305 (2014).

[26] Q. Meng and Y. Mo, Predissociation dynamics in the $3p\pi\ D\ ^1\Pi_u^{\pm}(\upsilon = 3)$ and $4p\sigma\ B''\ ^1\Sigma_u^+(\upsilon = 1)$ states of H_2 revealed by product branching ratios and fragment angular distributions, J. Chem. Phys. **144**, 154305 (2016).

[27] Q. Meng, J. Wang, and Y. Mo, Angle-resolved Beutler-Fano profile and dynamics for the predissociation of H_2, Phys. Rev. A **93**, 050501(R) (2016).

[28] J. Wang, Q. Meng, and Y. Mo, Oscillation of Branching Ratios between the $D(2s) + D(1s)$ and the $D(2p) + D(1s)$ Channels in Direct Photodissociation of D_2, Phys. Rev. Lett. **119**, 053002 (2017).

[29] J. Wang, Q. Meng, and Y. Mo, Electronic and tunneling predissociations in the $2p\pi C^1\Pi_u^{\pm}(\upsilon = 19)$ and $3p\pi D^1\Pi_u^{\pm}(\upsilon = 4, 5)$ states of D_2 studied by a combination of XUV laser and velocity map imaging, J. Phys. Chem. A **121**, 5785 (2017).

[30] S. H. Lin, Calculation of anisotropic photoionization cross sections. I. Hydrogen atom, Can. J. Phys. **46**, 2719 (1968).

[31] W. Demtröder, *Laser Spectroscopy, Basic Concepts and Instrumentation* (Springer-Verlag, Berlin, 2003).

[32] U. Fano, Effects of configuration interaction on intensities and phase shifts, Phys. Rev. **124**, 1866 (1961).

[33] H. Lefebvre-Brion and R. W. Field, *The Spectra and Dynamics of Diatomic Molecules*, rev. ed. (Academic Press, New York, 2004).

[34] M. Glass-Maujean and L. D. A. Siebbeles, Angular distribution of photofragments along a Fano profile, Phys. Rev. A **44**, 1577 (1991).